The PDZ Domain-binding Motif of the Human T Cell Leukemia Virus Type 1 Tax Protein Induces Mislocalization of the Tumor Suppressor hScrib in T cells.

Charlotte Arpin-André, Jean-Michel Mesnard

THE JOURNAL OF BIOLOGICAL CHEMISTRY VOL. 282, NO. 45, pp. 33132–33141, November 9, 2007

The PDZ Domain-binding Motif of the Human T Cell Leukemia Virus Type 1 Tax Protein Induces Mislocalization of the Tumor Suppressor hScrib in T cells*

Received for publication, March 15, 2007, and in revised form, August 3, 2007 Published, JBC Papers in Press, September 11, 2007, DOI 10.1074/jbc.M702279200

Charlotte Arpin-André and Jean-Michel Mesnard[1]

From the Centre d'études d'agents Pathogènes et Biotechnologies pour la Santé, Centre National de la Recherche Scientifique/UM 1/UM 2 UMR 5236/IFR 122, Institut de Biologie, 34965 Montpellier, France

Interactions with cellular PDZ domain-containing proteins obviously contribute to the tumorigenic potential of several viral oncoproteins. In this regard, the oncogenic potential of the human T cell leukemia virus type 1 Tax protein correlates with its binding capacity to the tumor suppressor hDlg. Recent results show that hDlg in T cells is associated to a network of scaffolding proteins including another PDZ domain-containing protein termed hScrib. Interestingly, previous studies have revealed complementary activities of both proteins in the control of epithelial cell polarity. Here, we demonstrate that Tax can bind to hScrib and that the resulting Tax/hScrib complex is present in human T cell leukemia virus type 1-infected T cells. By confocal microscopy, we show that Tax modifies the localization of hScrib in transfected COS cells as well as in infected T cell lines and targets hScrib to particular spots exhibiting a granular distribution, mainly distributed in the cytoplasm. Given that Tax sequesters hScrib to these particular structures, we postulate that Tax might inhibit hScrib activity. Providing further support to this idea, we find that transient overexpression of hScrib attenuates T cell receptor-induced NFAT activity but that the presence of Tax counteracts this negative effect on the NFAT pathway. The fact that hDlg and hScrib are both targeted by Tax underlies their importance in T cell function.

Adult T cell leukemia is caused by human T cell leukemia virus type 1 (HTLV-1)[2] infection and occurs several decades after initial infection (1). The viral protein Tax is considered to play a central role in the proliferation of infected cells and leukemogenesis because of its pleiotropic actions (2). During virus replication, Tax *trans*-activates viral transcription by interacting with different members of the activating transcription factor/cAMP-responsive element-binding protein (CREB), including ATF-1, CREB, CREB-2, or cAMP-responsive element modulator and by recruiting the transcriptional cofactors CREB-binding protein, p300, and P/CAF (3, 4). Tax also controls transcription of cellular genes by positively regulating different transcriptional pathways such as NF-κB, AP-1, and E2F or by negatively modulating others such as p53 and basic helix-loop-helix factors (5, 6). Thus, the oncogenic action of HTLV-1 likely involves deregulation of diverse cellular genes encoding proteins, which induce cell proliferation and inhibit apoptosis. Tax is also able to stimulate cell transformation by direct binding to cell cycle factors and deregulating checkpoints and DNA damage repair pathways (2, 7). Moreover, Tax contains a C-terminal PSD-95/SAP90, Discs Large, and Zona Occludens-1 (PDZ)-binding motif (PBM) (8), which has been shown to increase HTLV-1-induced proliferation of human peripheral blood mononuclear cells (9) and Tax-transforming activity in rat fibroblasts (10, 11). This enhanced transforming activity has been attributed to the interaction between Tax and the human homolog of the *Drosophila* discs large tumor suppressor (hDlg) (10, 12).

Dlg belongs to the family of proteins termed membrane-associated guanylate kinases (MAGUKs) (13). MAGUKs are characterized by the presence of distinct protein modules including the PDZ domain, SH3 domain, and guanylate kinase-like domain. MAGUKs act as molecular scaffolds (14) for cell polarity and signal transduction within epithelial cell junctions and neuronal synapses. Recently, hDlg has also been described to be involved in T cell polarity and immune synapse assembly (15, 16). Moreover, mutational studies in *Drosophila* have led to the classification of Dlg as a tumor suppressor (17). Its implication in cancer has been further supported by the demonstration that viral oncoproteins (adenovirus type 9 E4-ORF1, high risk human papillomavirus (HPV) E6, and Tax) target the cellular protein (18). hDlg has been shown to form a complex with APC (adenomatous polyposis coli) protein (19), which negatively regulates cell cycle progression (20). The *APC* gene is mutated in colon cancers, and the mutated gene product generally lacks the PBM (21). Moreover, the PBMs of Tax, HPV E6, and adenovirus type 9 E4-ORF1 interact with the same Dlg PDZ domain targeted by APC, suggesting that they may disrupt the APC-Dlg complex and deregulate cell cycle progression (12, 18, 22). However, the growth suppressing ability of Dlg cannot solely be attributed to its membrane-associated activity,

* This work was supported by institutional grants from the Centre National de la Recherche Scientifique and the Université Montpellier 1 and Association pour la Recherche sur le Cancer Grant 3606 (to J.-M. M.). The costs of publication of this article were defrayed in part by the payment of page charges. This article must therefore be hereby marked "*advertisement*" in accordance with 18 U.S.C. Section 1734 solely to indicate this fact.

[1] To whom correspondence should be addressed: Centre d'études d'agents Pathogènes et Biotechnologies pour la Santé, UMR 5236, Institut de Biologie, CS 69033, 4 Bd Henri IV, 34965 Montpellier Cedex 2, France. Tel.: 33-467-600-349; Fax: 33-467-604-420; E-mail: jean-michel.mesnard@univ-montp1.fr.

[2] The abbreviations used are: HTLV-1, human T cell leukemia virus type 1; CREB, cAMP-responsive element-binding protein; PDM, PDZ-binding motif; MAGUK, membrane-associated guanylate kinase; HPV, human papillomavirus; TCR, T cell receptor; NFAT, nuclear factor of activated T cells; GST, glutathione *S*-transferase; PBS, phosphate-buffered saline; HA, hemagglutinin; EGFP, enhanced green fluorescent protein; IS, immunological synapse.

because it has been demonstrated that the high risk HPV E6 protein targets the cytoplasmic and nuclear pools (23) of hDlg rather than membrane-associated forms (24).

Mutational studies in *Drosophila* have shown that Dlg act in concert with two other tumor suppressors, the Scrib (Scribble) and Lgl (lethal giant larvae) proteins, to regulate cell polarity and growth control (25). The three proteins are highly conserved in sequence among species and are likely functionally conserved as well (17). Scrib is a member of the LAP (leucine-rich and PDZ domain) family of proteins and possesses 16 canonical leucine-rich repeats and four PDZ domains (26). Scrib and Dlg form a scaffolding complex, whose function is required for the maintenance of correct epithelial polarity and efficient signal transmission at synaptic junctions (27). Reduction in hScrib expression in T cells prevents the polarization of cell surface receptors and morphological changes associated with uropod formation, migration, and antigen presentation (28). Interestingly, hScrib was first isolated in a biochemical screen designed to identify protein targets of HPV-39 E6, and it is now well established that the high risk HPV E6 proteins can target both hScrib and hDlg for proteasome-mediated degradation (29). Altogether these observations suggest the possible existence of a common mechanism underlying inhibition of two suppressor proteins by human viral oncoproteins. Moreover, by a two-hybrid approach, we have previously isolated different cDNAs encoding cellular proteins able to interact with Tax in yeast (30). Among them, we characterized clones containing cDNA corresponding to the human myeloblast KIAA0147 gene (GenBank^{TM} accession number D63481) coding for a protein of unknown function at this time (30). It was subsequently demonstrated that the KIAA0147 cDNA clone corresponds to an incomplete *hScrib* sequence (31), suggesting possible interactions of hScrib with Tax.

Here we demonstrate that Tax binds to hScrib and that this complex is present in HTLV-1-infected T cells. Furthermore, Tax altered the subcellular localization of hScrib in cotransfected COS cells as well as in HTLV-1-infected T cell lines. Moreover, we show that transient overexpression of hScrib attenuates T cell receptor (TCR)-induced activity of nuclear factor of activated T cells (NFAT) and that the presence of Tax counteracts this negative effect on the NFAT pathway. Altogether our results demonstrate that Tax targets another PDZ-containing cellular factor, hScrib, known to be associated with hDlg in scaffolding complexes involved in T cell signaling.

EXPERIMENTAL PROCEDURES

Plasmids and Antibodies—The pGEX constructs expressing various regions of hScrib fused to the *Schistosoma japonicum* glutathione *S*-transferase (GST) have already been described and were obtained from J. M. Huibregtse (29). For the two-hybrid assay in yeast, pAS-Tax and pAS-TaxΔPBM have previously been described (32). hScrib PDZ domain cDNAs fused to the GAL4 activation domain cDNA of the pACT2 vector were generous gifts from J. P. Borg (33). For transfection assays in COS and T cell lines, pSG-Tax, pSG-TaxM22, and pSG-TaxM47 (32, 34) have been used. pEGFP-Tax, pSG-Tax2, and pEGFP-Tax2 were obtained from R. Mahieux (35). The TaxΔPBM cDNA fragment was generated by PCR amplification using Deep Vent DNA polymerase, pSG-Tax as template, and specific sense and antisense primers (the six last amino acid residues of the wild type Tax sequence were deleted). The TaxΔPBM cDNA was inserted in-frame into the MluI/BamHI sites of the linearized pSG-Tax and into the EcoRI/BamHI cloning sites of the linearized pEGFP-C2 plasmid. pEGFP-hScrib (33) and pHA-hScrib (36) were obtained from J. P. Borg. pTxRE-Luc contains three tandem copies of the promoter-proximal TxRE and has already been described (32). The NFAT luciferase construct (pNFAT-Luc) contains a trimerized human NFAT site and was a gift from W. C. Greene.

The goat (C-20 and K-21) and rabbit anti-hScrib (H-300), goat anti-HP1α (C-15), mouse anti-HA (F-7) antibodies were purchased from Santa Cruz Biotechnology, Inc. (Santa Cruz, CA). The mouse anti-Myc antibody 9E10 has already been described (37). Anti-Tax was obtained through the AIDS Research and Reference Reagent Program of the Division of AIDS, NIAID, National Institutes of Health. HTLV-1 Tax hybridoma 168A51 (Tab176) was from B. Langton.

GST Pulldown Assay—pGEX vectors were transformed into *Escherichia coli* BL21 to produce GST fusion proteins, which were purified as described by the manufacturer (Amersham Biosciences). Then Tax or Tax2 cDNA cloned into pSG was transcribed and translated in the presence of [^{35}S]methionine using the TnT T7-coupled reticulocyte lysate system of Promega and incubated at 4 °C with equal amounts of GST immobilized on glutathione-Sepharose beads in a buffer containing 50 mM Tris-HCl, pH 7.4, 1 mM EDTA, 250 mM NaCl, 0.1% Nonidet P-40. After a 2-h incubation, the beads were washed five times with incubation buffer, and the bound proteins were analyzed by SDS-PAGE followed by autoradiography.

Two-hybrid Assay in Yeast—Study of interactions between Tax and hScrib PDZ domains was carried out by two-hybrid assay in *Saccharomyces cerevisiae* strain Y190 as previously described (34). Strain Y190 possesses the *E. coli lacZ* gene driven by the GAL4-responsive GAL1 promoter.

Protein Procedures—For Western blotting analysis of endogenous hScrib, uninfected or HTLV-1-infected cells (5×10^6) were concentrated by centrifugation, and the cell pellets were lysed in 50 mM HEPES, pH 7.5, 10% glycerol, 150 mM NaCl, 1 mM EGTA, 1.5 mM $MgCl_2$, 1% Triton X-100 supplemented with 1 mM phenylmethylsulfonyl fluoride, 10 μg/ml aprotinin, and 10 μg/ml leupeptin. Protein extracts were then electrophoresed on SDS-9% polyacrylamide gel and blotted to polyvinylidene difluoride membranes (Millipore). The blot was incubated 1 h at room temperature with a blocking solution (PBS, 0.1% Tween 20 containing 5% milk) prior to the addition of the goat anti-hScrib antibody (C-20). After 1 h, the blot was washed three times with PBS, 0.1% Tween 20 and incubated for 1 h with anti-goat immunoglobulin-peroxydase conjugate. After three washes, the membrane was incubated with ECL reagent (Amersham Biosciences). The membrane was then exposed to hyperfilms-ECL (Amersham Biosciences).

For immunoprecipitation of hScrib, uninfected or infected cells (5×10^6) were washed twice with PBS, and protein extracts were prepared as described above. The proteins were immunoprecipitated with 5 μg of antibodies from extracts (500 μg of total proteins) as already described (33). Bound fractions

were washed three times in lysis buffer containing 0.1% Triton and then electrophoresed on SDS, 9% polyacrylamide gel and analyzed by Western blotting.

Fluorescence Microscopy Analysis—COS cells were cultured in Dulbecco's modified Eagle's medium supplemented with 10% fetal calf serum. 24 h before transfection, the cells were seeded onto glass slides. For the transfections, we used the jet-PEI™ transfection reagent (Qbiogene) according to the manufacturer's instructions, and, after 48 h, they were washed with PBS, fixed, and permeabilized with 4% paraformaldehyde and 0.1% Triton X-100 for 30 min at room temperature. If necessary, the fixed cells were first incubated with a blocking solution (PBS containing 1% gelatin) and then with primary antibody for 1 h at room temperature. The samples were washed with PBS, 1% gelatin and then incubated with secondary antibody coupled to Texas Red (Pierce), Alexa Fluor 488, or Alexa Fluor 568 (Invitrogen) for 1 h at room temperature. The coverslips were mounted with Vectashield containing 4′,6′-diamino-2-phenylindole (Abcys) for direct observation. Fluorescence images were acquired by fluorescence microscope (model DM R; Leica), and analysis of the green, red, and yellow fluorescence for colocalization experiments was performed with a Bio-Rad MRC 1024 confocal microscope.

For CEM and HTLV-1-infected T cell lines, the cells were cultured in RPMI supplemented with 10% fetal calf serum. 10^7 cells were electroporated according to the previously published procedure (32). After 48 h, the cells were pelleted and washed twice in PBS, and one drop of concentrated cells was put down onto glass slides. Then the cells were fixed and permeabilized by treatment with cold methanol-acetone (1:1 v/v) for 5 min and incubated with primary antibody and with secondary antibody coupled to Red, Alexa Fluor 488, or Alexa Fluor 568 as already described. The coverslips were mounted with Vectashield without 4′,6′-diamino-2-phenylindole for observation by confocal microscope.

Transfection and Luciferase Assays—Jurkat cells (10^7) were electroporated as described above with the indicated quantities of pHA-hScrib (36) and 2 μg of NFAT reporter plasmid. 5 μg of pcDNA3.1-*lacZ* (β-galactosidase-containing reference plasmid) was included in each transfection for controlling of the transfection efficiency. The total amount of DNA in each transfection was the same, the balance being made up with empty plasmids. 48 h after transfection, half of the cells were stimulated for 6 h with mouse anti-human CD3 and anti-human CD28 monoclonal antibodies (Immunotech Beckman Coulter, Marseille, France) immobilized on a 6-well plate. The cells were then concentrated by centrifugation, resuspended in 100 μl of Passive Lysis Buffer (Promega), incubated in liquid nitrogen until frozen, and thawed at 4 °C. The cell extracts equalized for protein contents were used for luciferase and β-galactosidase assays, and the luciferase values were normalized for β-galactosidase activity. Luciferase assays were performed in an automated luminometer with the Genofax A kit (Yelen, Ensue la Redonne, France).

RESULTS

Tax Binds to the hScrib PDZ Domains 2 and 4 (PDZ2 and PDZ4)—In a previous yeast two-hybrid screening (30) performed with Tax as a bait, we isolated cDNA clones corresponding to the human myeloblast KIAA0147 gene (GenBank™ accession number D63481) that in fact encoded an incomplete *hScrib* sequence (31). hScrib contains a set of leucine-rich repeats near its N terminus and four PDZ domains (Fig. 1) distributed throughout the remainder of the protein (PDZ1 from residues 752 to 811, PDZ2 from residues 874 to 947, PDZ3 from residues 1015 to 1090, and PDZ4 from residues 1114 to 1189). The characterized clones corresponded to two different *hScrib* cDNAs, both coding for at least two PDZ domains (either PDZ1 + 2, or PDZ3 + 4), as shown in Fig. 1*A*.

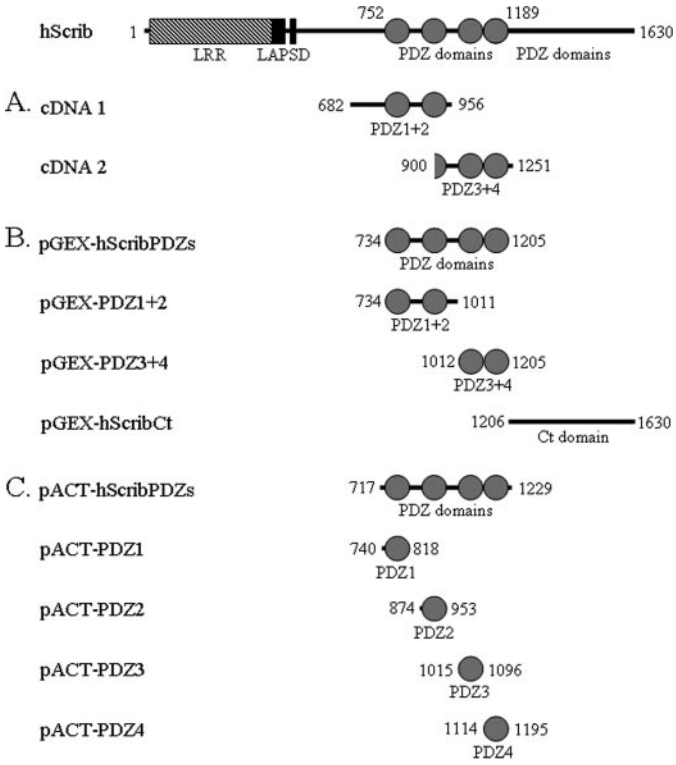

FIGURE 1. **Molecular structure of hScrib and its deletion mutants.** hScrib contains 16 leucine-rich repeats followed by two LAP-specific domain (*LAPSD*) and four PDZ domains. *A*, description of the two clones isolated by the yeast two-hybrid approach. *B* and *C*, structures of the hScrib constructs fused to the GST protein encoded by the pGEX vector (*B*) or fused to the GAL4 activation domain of the pACT2 vector (*C*). The *numbers* shown indicate amino acid positions.

To eliminate the possibility that the binding of Tax to hScrib PDZ domains may be indirect and dependent on yeast components, fusion proteins of various regions of hScrib with GST (Fig. 1*B*) were produced in *E. coli*, and their binding to ^{35}S-labeled Tax produced in rabbit reticulocyte lysate was analyzed. Tax bound to the hScrib domains corresponding to PDZ1 + 2 and PDZ3 + 4 (Fig. 2*A*), as already found by the two-hybrid approach. On the other hand, Tax did not significantly interact with the negative control corresponding to the hScrib C-terminal region fused to GST (Fig. 2*A*). We also analyzed the interaction between the hScrib PDZ domains and a Tax mutant without its PBM. This mutant was effectively unable to bind to the PDZ domains (data not shown). Moreover, we also found no interaction between the hScrib PDZ domains and the HTLV-2 Tax protein, Tax2 (Fig. 2*A*), which does not possess a C-terminal PBM (9).

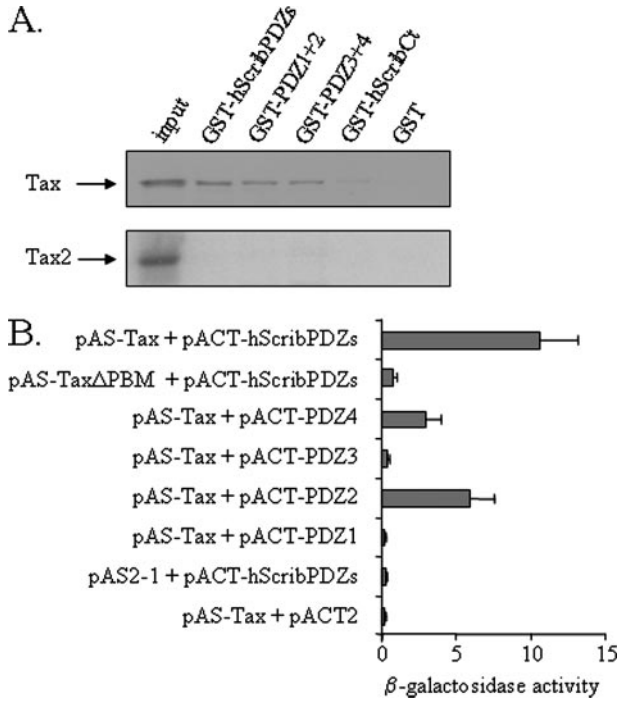

FIGURE 2. **Tax binds to the hScrib PDZ2 and PDZ4.** *A*, *in vitro* binding assays of Tax to the PDZ domains of hScrib. Equal amounts of GST and GST fused to the PDZ domain region (hScribPDZs, PDZ1 + 2, PDZ3 + 4) or to the C-terminal domain (hScribCt) of hScrib were immobilized on glutathione-Sepharose beads, incubated with [^{35}S]Tax or [^{35}S]Tax2 (input), and bound proteins were analyzed by SDS-PAGE and autoradiography. *B*, analysis of the interactions between Tax and the different PDZ domains of hScrib using a liquid culture β-galactosidase assay. Yeasts were transformed with the expression vector pAS2-1 containing the entire coding sequence of Tax or that of a Tax mutant without PBM (TaxΔPBM), fused to the GAL4 DNA-binding domain, together with pACT-2, expressing the GAL4 activation domain fused to the different hScrib PDZ domains. The β-galactosidase assay with *o*-nitrophenyl-β-D-galactopyranoside as substrate was carried out on three independent colonies per transformation as described in the Clontech protocol. The values, expressed in Miller units, represent the means ± S.D. ($n = 3$).

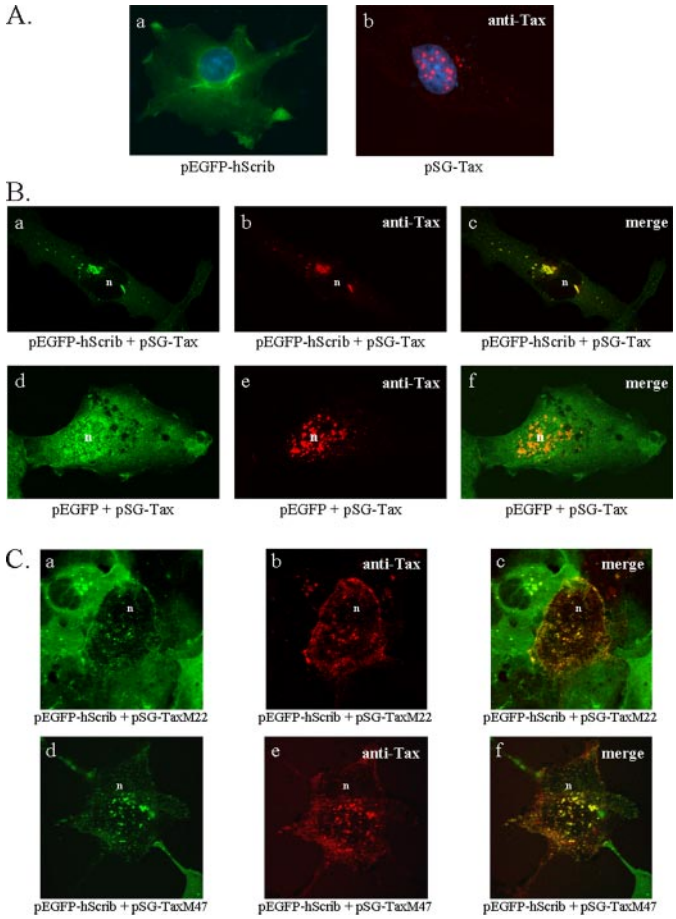

FIGURE 3. **Microscopy analysis of the colocalization of Tax and hScrib *in vivo*.** *A*, fluorescence microscopy analysis of the cellular localization of hScrib *in vivo*. COS cells transfected with pEGFP-hScrib (*panel a*) or pSG-Tax (*panel b*) were cultivated on glass slides, fixed, and treated with Vectashield containing 4′,6′-diamino-2-phenylindole for direct characterization of the nucleus by fluorescence microscopy. The Tax protein (*panel b*) was detected by using the anti-Tax antibody and goat anti-mouse immunoglobulin G antibody coupled to Texas Red. *B*, confocal microscopy analysis of the colocalization of hScrib and Tax *in vivo*. Analysis of green (*panel a* and *d*), red (*panel b* and *e*), and merged (*panel c* and *f*) fluorescence was performed with a confocal microscope for COS cells cotransfected with pSG-Tax and pEGFP-hScrib (*panels a–c*) or with pSG-Tax and the empty vector pEGFP as negative control (*panel d–f*). The Tax protein was detected as described above. *C*, colocalization of EGFP-hScrib with the Tax mutants M22 and M47. Analysis of green (*panels a* and *d*), red (*panels b* and *e*), and merged (*panels c* and *f*) fluorescence was performed with a confocal microscope. *n*, nucleus.

Our results show that Tax is capable of interacting with hScrib PDZ domains *in vitro*. To map more precisely the Tax-binding domain of hScrib, each PDZ domain fused to the GAL4 activation domain of the pACT2 plasmid (Fig. 1*C*) was tested for interaction with Tax by two-hybrid assay in yeast. As shown in Fig. 2*B*, Tax bound to PDZ2 and PDZ4. We also analyzed the interaction between the hScrib PDZ domains and the Tax mutant without its PBM, TaxΔPBM. This mutant was effectively unable to bind to the PDZ domains (Fig. 2*B*). In conclusion, these data indicate that the hScrib PDZ2 and PDZ4 are the targets of Tax.

Tax Interacts with hScrib in Vivo—To confirm the *in vivo* relevance of the binding of Tax to hScrib, the subcellular localization of both proteins expressed either separately or together was examined in transfected COS cells by immunofluorescence microscopy. As previously described, Tax was shown to be localized in the cytoplasm as well as the nucleus (35, 38) (Fig. 3*A*). On the other hand, EGFP-hScrib mainly showed a diffuse pattern in the cytoplasm, whereas only a small proportion was found to be cell membrane-associated (Fig. 3*A*). A similar pattern has been observed for Erbin (a cellular protein also containing both leucine-rich repeat and PDZ domains) in HeLa cells transfected by pEGFP-Erbin (39). However, when hScrib was cotransfected with Tax, the staining pattern of hScrib was modified because both proteins colocalized in particular spots exhibiting a granular distribution (100% of cotransfected cells), mainly in the cytoplasm (Fig. 3*B*). On the other hand, Tax did not modify the staining pattern of the EGFP control (Fig. 3*B*). Interestingly, the presence of EGFP-hScrib can also change the subcellular localization of Tax, suggesting that hScrib might have affected some Tax functions. In conclusion, our observations support the notion that Tax and hScrib interact *in vivo* and that Tax might entail a subcellular redistribution of hScrib.

To be sure that other cellular Tax-binding proteins are not involved, the subcellular localization of hScrib was examined in the presence of different Tax mutants. COS cells were first cotransfected with pEGFP-hScrib and pSG-TaxM22 or pSG-TaxM47. M22 and M47, respectively, are NF-κB-defective or CREB-defective Tax mutants, but both mutants contain the

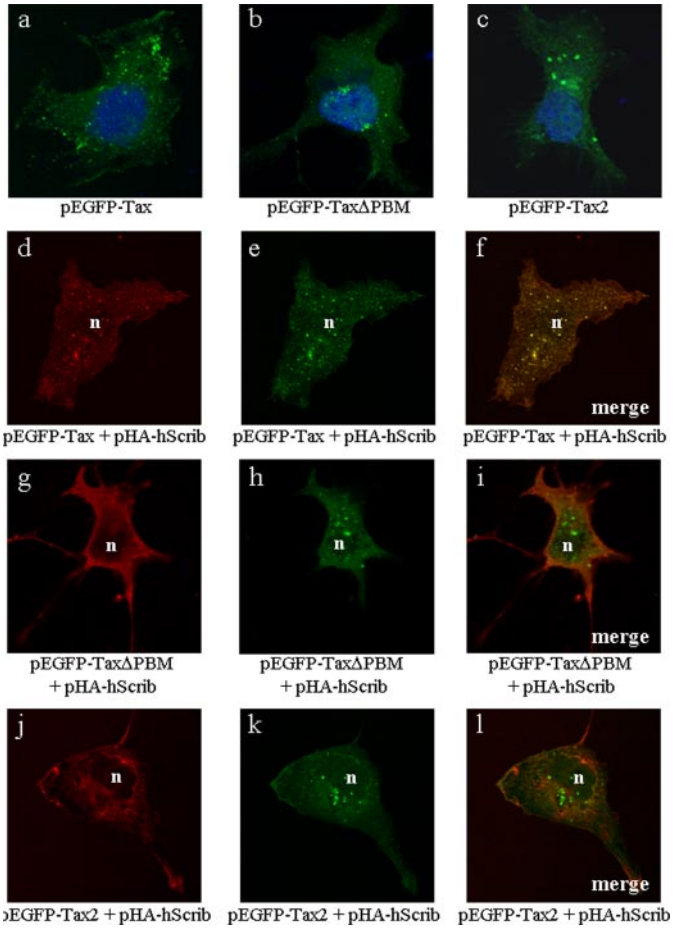

FIGURE 4. **The PBM of Tax is necessary for mislocalization of hScrib in transfected COS cells.** Cells were transfected with pEGFP-Tax (*panel a*), pEGFP-TaxΔPBM (*panel b*), and pEGFP-Tax2 (*panel c*) in the presence of pHA-hScrib (*panel d–l*). HA-hScrib was detected by using the anti-HA antibody and goat anti-mouse immunoglobulin G antibody coupled to Alexa Fluor 568. Analysis of green (*panels d*, *g*, and *j*), red (*panels e*, *h*, and *k*), and merged (*panels f*, *i*, and *l*) fluorescence was performed by confocal microscopy. *n*, nucleus.

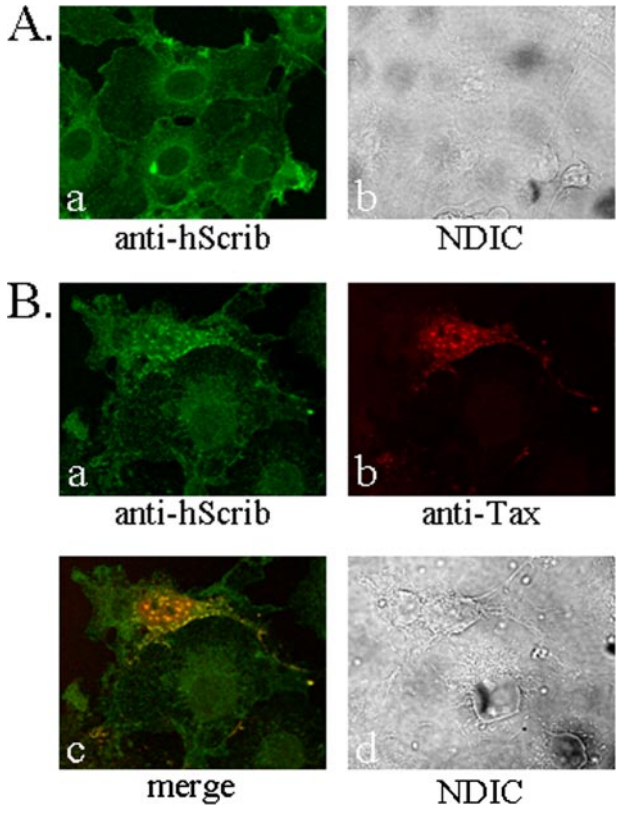

FIGURE 5. **Tax alters subcellular localization of endogenous hScrib.** *A*, confocal microscopy analysis of endogenous hScrib. COS cells were stained with the rabbit anti-hScrib antibody and goat anti-rabbit immunoglobulin G antibody coupled to Alexa Fluor 488 (*panel a*). The morphology of cells (*panel b*) was characterized by Normaski differential interference contrast (*NDIC*). *B*, colocalization of endogenous hScrib and Tax in COS cells transfected with pSG-Tax. For localization observation of endogenous hScrib in the presence of Tax, analysis of green (*panel a*), red (*panel b*), and merged (*panel c*) fluorescence was performed with a confocal microscope. The Tax protein was detected by using the anti-Tax antibody and goat anti-mouse immunoglobulin G antibody coupled to Alexa Fluor 568.

C-terminal PBM. As shown in Fig. 3*C*, the staining pattern of hScrib can also be modified in the presence of both mutants, still exhibiting a granular distribution. These results demonstrate that M22 and M47 are also able to modify the localization of hScrib in transfected COS cells.

We next studied the intracellular distribution of hScrib in the presence of TaxΔPBM and Tax2, which does not interact with hScrib. However, when the last six C-terminal amino acid residues of Tax were deleted, our anti-Tax antibody was no longer able to detect the Tax mutant in transfected cells (data not shown). As a previous report demonstrated that EGFP-Tax and EGFP-Tax2 have the same cellular distribution as the non-tagged Tax proteins (35), we hypothesized that EGFP-Tax, -TaxΔPBM, and -Tax2 could be used for analyzing their interactions with HA-tagged hScrib (36). Effectively, as shown in Fig. 4 (*panels d–f*), EGFP-Tax and HA-Scrib colocalized in spots formed by the viral protein. On the other hand, the staining pattern of the HA-Scrib was not modified in the presence of EGFP-TaxΔPBM (Fig. 4, *panels g–i*) and EGFP-Tax2 (Fig. 4, *panels j–l*).

Having demonstrated that Tax can interact with hScrib, we also examined the subcellular localization of endogenous hScrib in the absence and the presence of Tax. In the absence of Tax, endogenous hScrib was present in the cytoplasm and on the membrane (Fig. 5*A*). On the other hand, in the presence of Tax (Fig. 5*B*), endogenous hScrib colocalized with Tax in particular spots. Taken together, our results indicated that Tax is able to sequester hScrib within Tax-containing complex.

Tax Interacts with hScrib in T Cells—Next, to confirm that endogenous Tax and hScrib were effectively associated in infected T cells, immunoprecipitations of cell lysates of HTLV-1-infected cell lines (HUT102 and C8166) were performed with a goat anti-hScrib antibody, and the immunoprecipitates were probed with an anti-Tax monoclonal antibody. As expected, this approach revealed the presence of a complex between Tax and hScrib in HUT102 and C8166 extracts (Fig. 6*A*), but not in the uninfected CEM cell line (Fig. 6*B*). By the same approach but using a goat anti-HP1α as control, we did not immunoprecipitate Tax (Fig. 6, *A* and *B*). We also performed reverse immunoprecipitations of extracts of infected (C8166) and uninfected (CEM) cells by using the anti-Tax antibody and by probing the immunoprecipitates with the goat anti-hScrib antibody. hScrib coprecipitated with Tax, but it did not precipitate with material

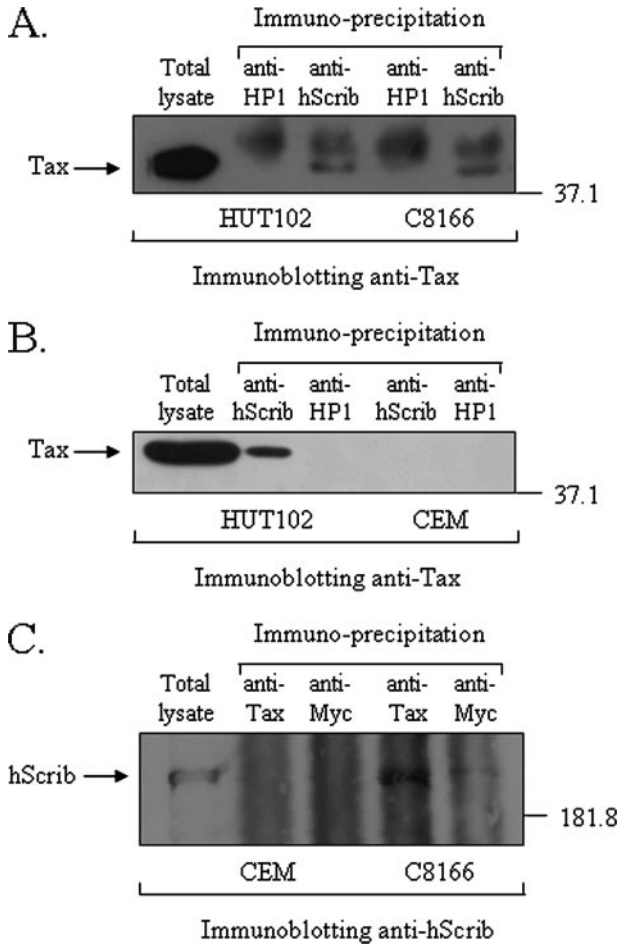

FIGURE 6. **Tax-hScrib association in the HUT102 and C8166 cell lines.** *A* and *B*, proteins from the total lysate of HTLV-1-infected HUT102 cells were directly probed with mouse anti-Tax (*first lane*, total lysate) or immunoprecipitated with goat anti-hScrib (*lanes anti-hScrib*) or goat anti-HP1α (*lanes anti-HP1*) antibodies followed by Western blot analysis with anti-Tax. Immunoprecipitation and Western blotting were also performed in the same conditions with HTLV-1-infected C8166 (*A*) and uninfected CEM (*B*) cells. *C*, extracts of CEM were also directly probed with goat anti-hScrib (*first lane*, total lysate) or immunoprecipitated with mouse anti-Tax (*lanes anti-Tax*) or mouse anti-Myc (*lanes anti-Myc*) antibodies followed by Western blot analysis with goat anti-hScrib. The same approach was also performed with C8166 extracts (*C*). The molecular mass markers (in kilodaltons) are indicated on the *right* of the figure.

recovered using the control antibody (Fig. 6*C*). In conclusion, our results clearly demonstrate that Tax and hScrib interact in HTLV-1-infected T cells.

Tax Modifies hScrib Activity in T Cells—Although the exact mechanism of action of the PDZ-containing proteins (such as hScrib and hDlg) remains unclear in T cells, their involvement in T cell signaling has been suggested (28). Moreover, it has been recently demonstrated that overexpression of hDlg affected CD3-potentiated NFAT activation in Jurkat cells (15, 16). For all these reasons, it was of high interest to test the effects of hScrib on NFAT activity after stimulation of T cell activation. Therefore, Jurkat cells were first cotransfected with an NFAT reporter construct in the presence of increasing amounts of a HA-tagged hScrib expression vector (pHA-hScrib) and then stimulated with anti-human CD3 combined with anti-human CD28. As shown in Fig. 7*A* and as already described for hDlg (16), overexpression of hScrib attenuated NFAT reporter activity in stimulated Jurkat cells. On the other hand, cotransfection of Tax expression vector (pSG-Tax) restored the CD3/CD28-potentiated NFAT activation (Fig. 7*B*). Interestingly, cotransfection of increasing amounts of pHA-hScrib resulted in diminution of Tax effect (Fig. 7*B*). In the same way, cotransfection of increasing amounts of pSG-Tax in the presence of an unchanged amount of hScrib resulted in a significant increase in luciferase activity (Fig. 7*C*). However, it was interesting to determine whether the negative effect could be reciprocal as suggested by confocal microscopy analyses shown in Fig. 3. For this reason, the transcriptional activity of Tax was measured in the presence of hScrib by using TxRE-Luc, a Tax-responsive luciferase reporter construct that contains three tandem copies of the promoter-proximal TxRE. Fig. 7*D* clearly shows that increasing amounts of hScrib inhibited the Tax *trans*-activation of the promoter-proximal TxRE. This negative effect of hScrib on Tax-dependent transcription confirms that both proteins interact *in vivo*.

However, to be sure that the observed effects of Tax and hScrib on the NFAT reporter construct are not due to independent activities, we also analyzed the effects of the mutant TaxΔPBM. Therefore, we compared the activities of the Tax, TaxΔPBM, TaxM22, and TaxM47 on NFAT reporter plasmid after stimulation of T cell activation. In the absence of hScrib (Fig. 8*A*), all of the mutants except M47 were able to enhance NFAT activity. It is noteworthy that M47 is known to be unable to recruit multifunctional cellular coactivators such as CREB-binding protein, p300, or P/CAF (6). On the other hand, in the presence of hScrib (Fig. 8*B*), whereas Tax was capable of restoring the CD3/CD28-potentiated NFAT activation, the mutant TaxΔPBM was unable. Moreover, M22 was not as efficient as the wild type Tax. In addition to being deficient in NF-κB activation, M22 has also been described to be impaired in Tax self-association (34). Because we have demonstrated that Tax can interact with hScrib PDZ2 and PDZ4, it is possible that Tax dimerization might favor interactions with the different PDZ domains. However, for the moment, we cannot confirm this hypothesis, and further studies are still necessary to explain this result with M22. Taken together, our results suggest that Tax is able to down-regulate the hScrib activity *in vivo* via its PBM.

Tax Colocalizes with hScrib in HTLV-1-infected Cell Lines—It has been recently demonstrated that Tax negatively controls the activity of another tumor suppressor, the retinoblastoma protein. Tax targets the retinoblastoma protein for proteasomal degradation and thus decreases its level in infected T cells (40). We could not exclude this possibility in the case of hScrib, and then we examined the status of hScrib in HTLV-1-infected T cell lines known to express Tax such as MT4, C8166, and HUT102 cell lines. As shown in Fig. 9, no significant difference was observed in hScrib expression in the HTLV-1-infected cell lines as compared with uninfected CEM, Jurkat, and H9 cells. Moreover, to determine whether Tax could be responsible for hScrib degradation, we also analyzed the stability of hScrib in the presence of increasing amount of Tax by transient cotransfection assays. Again, we were unable to observe a significant effect of Tax on hScrib expression (data not shown).

Given our results on the relocalization of hScrib in the presence of Tax in cotransfected COS cells, we next hypothesized

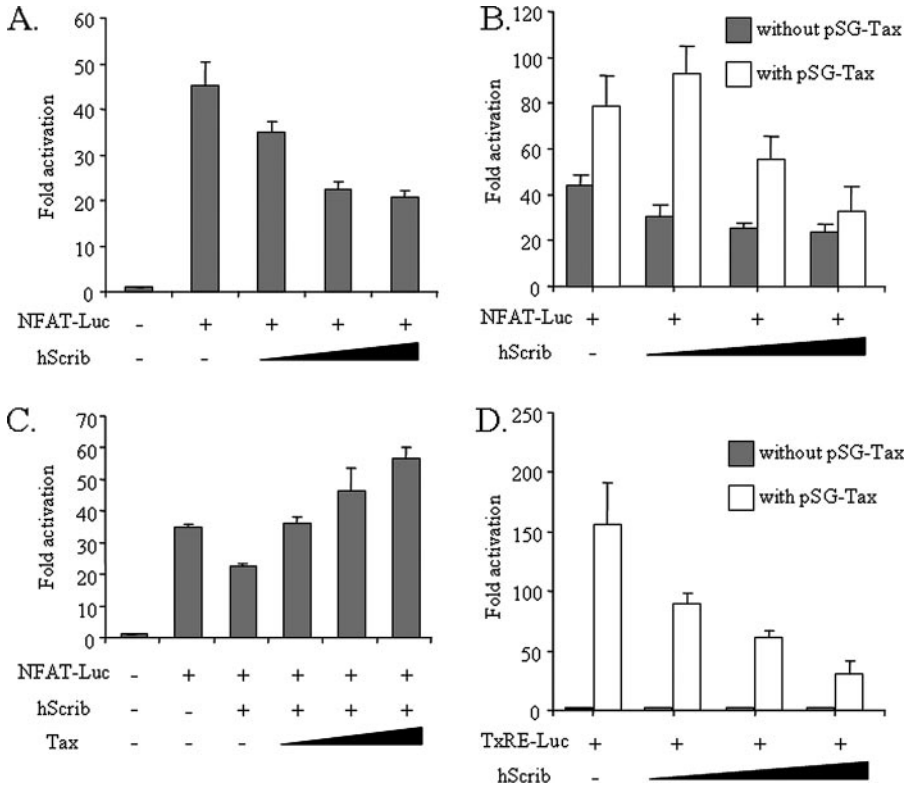

FIGURE 7. **Effects of hScrib expression on transcriptional activity in Jurkat cells.** *A*, overexpression of hScrib attenuates NFAT transcriptional activity in Jurkat cells stimulated with anti-human CD3 combined with anti-human CD28. Activated Jurkat cells were cotransfected with 2 μg of pNFAT-Luc, 5 μg of pcDNA3.1lacZ (β-galactosidase-containing reference plasmid), and pHA-hScrib (0, 1, 2, or 5 μg). The luciferase values are expressed as fold increase relative to that of cells transfected with a luciferase reporter construct carrying no NFAT site. The total amount of DNA in each series of transfection was equal, the balance being made up with the empty plasmids, and the luciferase values were normalized for β-galactosidase activity. The values represent the means $\pm$ S.D. ($n = 3$). *B*, effect of Tax on hScrib-induced repression of NFAT activity. Jurkat cells were cotransfected in the same conditions as described above in the presence or not of 1 μg of Tax expression vector pSG-Tax. The values represent the means $\pm$ S.D. ($n = 3$). *C*, effect of increasing amounts of Tax on hScrib-induced repression of NFAT activity. Activated Jurkat cells were cotransfected with 2 μg of pNFAT-Luc, 3 μg of pHA-hScrib, and pSG-Tax (0, 0.2, 0.5, or 1 μg). The values represent the means $\pm$ S.D. ($n = 3$). *D*, hScrib down-regulates Tax-dependent transcription. Jurkat cells were cotransfected with 2 μg of HTLV-1 TxRE-Luc and pHA-hScrib (0, 1, 2, or 5 μg) in the presence or absence of 1 μg of pSG-Tax. The luciferase values are expressed as increases relative to that of cells transfected with TxRE-Luc in the presence of the empty plasmids. The values represent the means $\pm$ S.D. ($n = 3$).

that Tax could also induce a mislocalization of hScrib in HTLV-1-infected T cells. We first performed this study with T cell lines transfected with EGFP-tagged constructs. Indeed, EGFP-hScrib is known to colocalize with endogenous hScrib (36). In addition, by this approach, it was possible to compare the localization of the wild type protein with that of the hScribΔPDZs mutant (this mutated form of hScrib does not interact with Tax) in HTLV-1-infected cell lines. We also analyzed hScrib distribution and subcellular localization of EGFP-hScrib and EGFP-hScribΔPDZs in the uninfected CEM cell line by confocal microscopy (Fig. 10, *panels a–d*). As already described for hDlg in Jurkat cells (16), EGFP-hScrib showed a diffuse cytoplasmic pattern. On the other hand, in the HTLV-1-infected C8166 (Fig. 10, *panels e–h*) and HUT102 (Fig. 10, *panels m–p*) cell lines, the staining pattern was different because EGFP-hScrib colocalized with endogenous Tax in particular spots exhibiting a granular distribution (80% of transfected cells), mainly in the cytoplasm. These data confirm our previous observations in COS cells cotransfected with pEGFP-hScrib and pSG-Tax (Fig. 3). Interestingly, when the same approach was performed with EGFP-hScribΔPDZs (Fig 10, *panels i–l* and *q–t* for C8166 and HUT102, respectively), the mutated protein was diffusely distributed throughout the cytoplasm. On the other hand, endogenous Tax remains mainly located in the nucleus (Fig. 10, *panels j* and *r*) with a staining pattern identical to that observed in untransfected C8166 and HUT102 cells (Fig. 11). These results confirm the involvement of the hScrib PDZ domains in the interaction with Tax.

Lastly, we analyzed the distribution of endogenous hScrib and Tax in the HTLV-1-infected C8166 (Fig. 11, *panels a–d*) and HUT102 (Fig. 11 *panels e–h*) cell lines. We observed that Tax partially colocalizes with hScrib in the cytoplasm (*arrows* indicate structures where Tax colocalizes with hScrib). Therefore, our observations demonstrate that Tax can bind to hScrib in HTLV-1-infected T cell lines, and this interaction entails a targeting of hScrib to particular bodies, mainly distributed in the cytoplasm.

DISCUSSION

The transforming activity of Tax in the Rat 1 fibroblast cell line has been shown to depend on its C-terminal PBM (10, 11). This motif is also necessary to promote HTLV-1-induced proliferation of human peripheral blood mononuclear cells (9). It has been demonstrated that Tax PBM mediates the interaction of the viral protein with the tumor suppressor hDlg (12). Through this interaction, Tax alters the subcellular localization of hDlg in 293T cells as well as in HTLV-1-infected T cells (10). Here, we demonstrate that Tax interacts *in vitro* and *in vivo* with a second human homolog of a *Drosophila* tumor suppressor, hScrib. Like hDlg, hScrib interacts with the C terminus of Tax via its PDZ domains, more precisely the PDZ2 and PDZ4 domains. In addition, our results show that, in COS cells and in the HTLV-1-infected T cell lines C8166 and HUT102, Tax directly binds to hScrib and modifies its subcellular localization. Findings presented in this paper also suggest that Tax is able to perturb hScrib activity. Interestingly, the PDZ2 domain of the *Drosophila* Scrib homolog has been found to be required for its proper localization and function in neuroblasts (41). In the same way, Tax interaction with the hDLG PDZ domain-containing region is also responsible for inhibition of hDlg activity in cotransfected NIH3T3 cells (12). Taken together, all of these data sug-

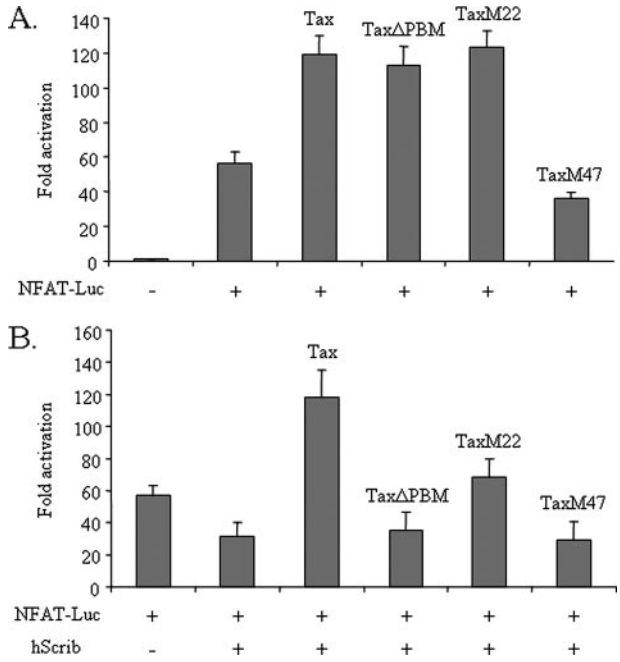

FIGURE 8. **Effects of TaxΔPBM, TaxM22, and TaxM47 on the CD3/CD28-induced NFAT activation in the absence (*A*) or in the presence (*B*) of hScrib.** To test the effects of the different Tax mutants on the pNFAT-Luc, Jurkat cells were transfected and stimulated as described in the legend of Fig. 7, with 1 μg of Tax-expression vector and 3 μg of pHA-hScrib. The values represent the means $\pm$ S.D. ($n = 3$).

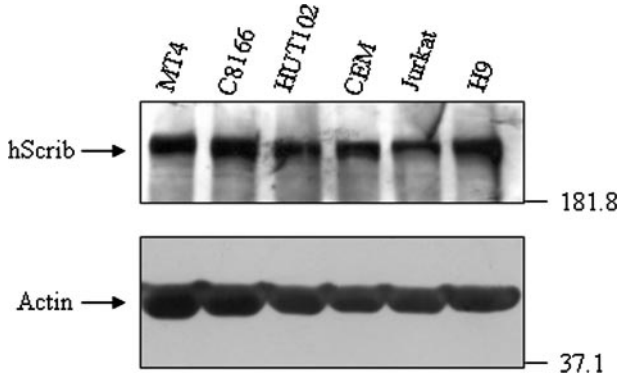

FIGURE 9. **Immunoblot analysis of crude extracts prepared from HTLV-1-infected (MT4, C8166, and HUT102) or uninfected (CEM, Jurkat, and H9) T cell lines.** Protein extracts were electrophoresed on a SDS, 9% polyacrylamide gel and analyzed by Western blotting using anti-hScrib (*top panel*) or anti-actin antibodies (*bottom panel*), immunoblotting against actin being used as a loading control. The molecular mass markers (in kilodaltons) are indicated on the *right* of both panels.

gest that Tax might inhibit hDlg and hScrib activities by altering their subcellular localization through interactions with their PDZ domains.

Other oncoproteins encoded by tumorigenic viruses have been found to interact with hDlg or hScrib (18, 22, 29). For example, the high risk tumor-promoting HPV-16 and HPV-18 E6 proteins also bind to both hDlg and hScrib and stimulate their degradation (29, 42). Moreover, PDZ binding activity of E6, which is distinct from the ability of E6 to bind and degrade p53, is important for cell transformation and has been shown to be necessary for the stimulation of epithelial hyperplasia in transgenic animals (43). The fact that Tax and E6 target hDlg and hScrib is consistent with the possibility that both PDZ

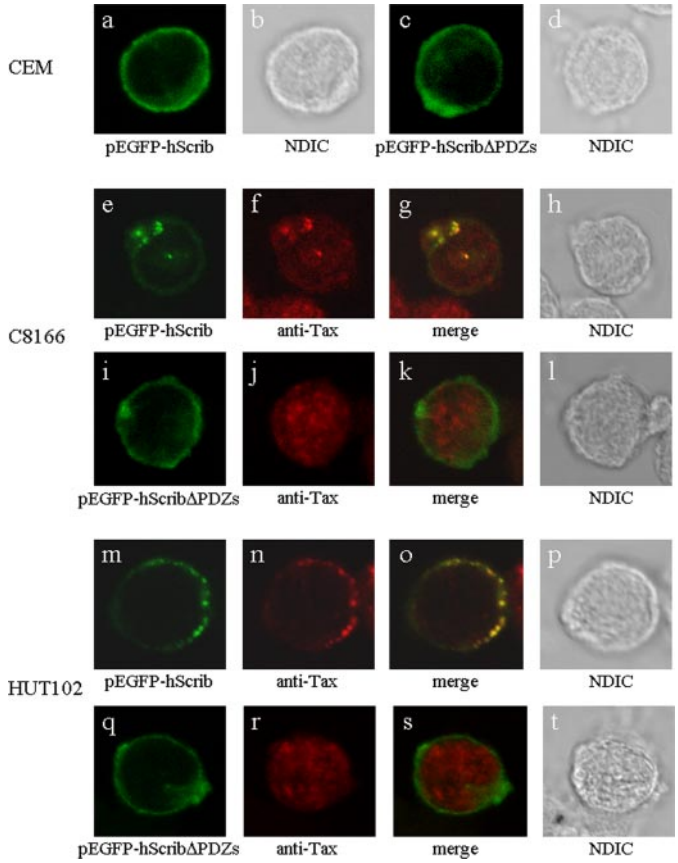

FIGURE 10. **Tax alters subcellular localization of hScrib in HTLV-1-infected T cell lines (C8166 and HUT102).** CEM cells (*panels a–d*) were transfected with pEGFP-hScrib (*panels a* and *b*) or pEGFP-hScribΔPDZs (*panels c* and *d*), cultivated on glass slides, and fixed, and the analysis of green fluorescence (*panels a* and *c*) was performed by confocal microscopy; the morphology of transfected cells (*panels b* and *d*) was characterized by Normaski differential interference contrast (*NDIC*). For colocalization observation of endogenous Tax with EGFP-hScrib in transfected C8166 (*panels e–h*) and HUT102 (*panels m–p*) cells, analysis of green (*panels e* and *m*), red (*panels f* and *n*), and merged (*panels g* and *o*) fluorescence was also performed with a confocal microscope. The Tax protein was detected by using the anti-Tax antibody and goat anti-mouse immunoglobulin G antibody coupled to Texas Red. As a negative control, the same approach was performed with C8166 (*panels i–l*) and HUT102 (*panels q–t*) cells transfected with pEGFP-hScribΔPDZs.

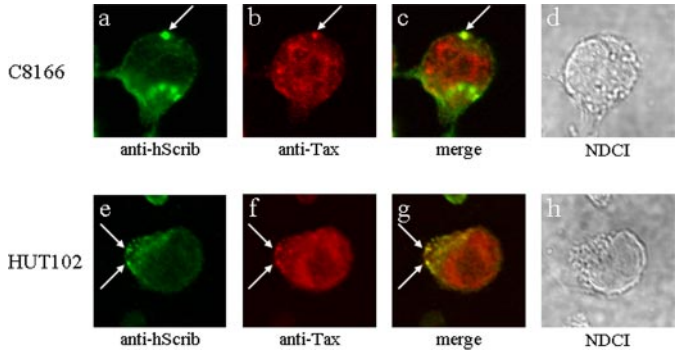

FIGURE 11. **Colocalization of Tax and hScrib in HTLV-I infected cells.** C8166 and HUT102 cells were stained for hScrib (*green*) and Tax (*red*) as already described in the legend of the Fig. 5, except we used the goat anti-hScrib antibody K-21 of Santa Cruz Biotechnology Inc. to detect endogenous hScrib. Colocalizations of Tax with hScrib are in *yellow*, highlighted by *arrows*. *NDCI*, Normaski differential interference contrast.

domain-containing proteins cooperate in an analogous pathway in mammalian cells. Viral oncoproteins might target both proteins to exert their biological effects by blocking the formation of multiprotein complexes containing hDlg and hScrib involved in the control of cell proliferation. In *Drosophila*, anatomical and biochemical experiments have shown that Dlg and Scrib form a complex with the GUKH (GUK holder) protein at neuromuscular junctions (27). It has been proposed that the binding of GUKH to the GUK domain of Dlg could cause sterical changes in GUKH, which would result in the exposure of the PBM for interaction with the second PDZ domain of Scrib (27). This study provides evidence that Dlg and Scrib may be directly associated to form a network of multiprotein complexes in insect cells involved in the regulation of synapse formation. However, for the moment, such a protein capable of linking hDlg and hScrib in a common complex has not been yet characterized in mammalian cells. Of course, APC has been described to interact with human homologs of both *Drosophila* tumor suppressors (20, 44), but, in this case, the PDZ domains of hScrib and hDlg are probably competing for the interaction with the C-terminal PBM of APC. The APC-hDlg complex is involved in the negative regulation of cell cycle progression from G_0/G_1 to S phase (20), and Tax is able to block this inhibitory effect by disrupting the complex between APC and hDlg (12). On the other hand, the role of the interaction between hScrib and APC still remains unclear, although it has been found that this association is essential for the structure of the adherens junction in epithelial cells (44). Adherens junctions connect adjacent cells and are known to play a role in cell-to-cell communications. Loss of junction integrity has been linked to tumor development, providing a hypothetical link between the degradation of hScrib and hDlg by the high risk E6 protein and the development of cervical cancer. In the same way, the Tax transforming activity in the Rat 1 fibroblast cell line might also be explained by the loss of cell contact inhibition due to the mislocalization of hDlg caused by its interaction with Tax (10). However such a mechanism does not really explain why Tax PBM promotes T cell proliferation (9).

T cell proliferation requires cell polarization, which involves morphological changes that are dictated by the recruitment of surface receptor, signaling complexes, and cellular organelles to discrete functional domains, such as the immunological synapse (IS) and the uropod (45, 46). IS formation starts with the binding of peptide-major histocompatibility complex complexes to TCRs and results in a change of polarity of the T cell, with recruitment of proteins such as Ezrin and CD43 to the distal pole of the cell and translocation of the microtubule organizing center to the IS. In addition, IS formation induces a complex series of signaling events that leads to the activation of T cells. Because the cytoplasmic tails of both TCR α and β chains have no signaling capacity, intracellular signals derive mainly from associated CD3 molecules and partially from accessory molecules like CD8/CD4 and costimulatory molecules, such as CD28. Two of the first molecules to be activated downstream of the TCR are the Src family tyrosine kinases $p56^{lck}$ (Lck) and $p59^{fyn}$ (Fyn), which catalyze phosphorylation of other molecules and lead to downstream signaling cascades, resulting in an increase of cytoplasmic Ca^{2+} and the activation of transcription factors, including NF-AT, NF-κB, and AP-1. Many observations have suggested that HTLV-1-infected T cells exhibit altered expression or activity of key molecules implicated in T cell activation (for instance, the modulation of the TCR-CD3 complex (47), the absence of Lck expression (48), and the overexpression of FynB (49)). Interestingly, hDlg directly interacts with Lck in T lymphocytes (50), and it has been suggested that, through this interaction, hDlg could coordinate phosphorylation of others molecules by Lck (15). Moreover, although many of molecular scaffolds and signals involved in T cell polarization have been elucidated, the exact mechanism by which T cell polarity is regulated is a matter of speculation. An interesting possibility for the regulation of T cell polarity and morphology during IS formation has been recently suggested and involves a network of PDZ-containing proteins, including hScrib and hDlg (28). In addition, the polarization network integrates cell shape with signaling by influencing the localized activity of signaling molecules. Indeed, it has been demonstrated that hDlg can regulate the activation of NFAT (15, 16). In this study, we show that hScrib has a similar effect on this transcription factor because its overexpression attenuated NFAT reporter activity in anti-CD3/anti-CD28-stimulated Jurkat cells. Interestingly, reduction in hDlg expression resulted in an increase of NFAT activation, leading to the conclusion that hDlg could act as a negative regulator of T cell signaling (16). Thus, by interacting with hScrib and hDlg, Tax could counteract this negative effect on NFAT activation and then stimulate T cell proliferation. However, for the moment, the mechanism by which hDlg and hScrib negatively controls the NFAT pathway remains completely unknown, and for this reason, additional data must be accumulated to confirm this hypothesis.

In conclusion, we show herein that, in addition to hDlg, hScrib is also targeted by Tax. This suggests that the interaction of both PDZ domain-containing proteins with Tax may dysregulate transmembrane signaling, although altered signaling would seem more likely to disrupt rather than activate proliferation signals. The exact molecular mechanism by which hDlg and hScrib control T cell signaling is presently unclear. A second scenario recently suggested by Frese *et al.* (51) may be more attractive and argues that the oncogenic activity of hDlg depends on the presence of the viral oncoprotein E4-ORF1. Future studies will be aimed at the characterization of the precise function of hScrib and hDlg in T lymphocytes to understand the possible links between their association with Tax and T cell proliferation.

Acknowledgments—We thank J.-P. Borg and J. M. Huibregtse for the kind gift of the different vectors encoding hScrib. We also thank R. Mahieux for the kind gift of pEGFP-Tax, pSG-Tax2, and pEGFP-Tax2, and we thank W. C. Greene for pNFAT-Luc. We thank B. Barbeau for critical reading of the manuscript. Confocal microscopy was performed by the Service de Cytométrie at the Centre Régional d'Imagerie Cellulaire in Montpellier.

REFERENCES

1. Takatsuki, K. (2005) *Retrovirology* **2,** 16
2. Grassmann, R., Aboud, M., and Jeang, K.-T. (2005) *Oncogene* **24,** 5976–5985

3. Lemasson, I., Polakowski, N. J., Laybourn, P. J., and Nyborg, J. K. (2002) *J. Biol. Chem.* **277,** 49459–49465
4. Mesnard, J.-M. (2005) in *Progress in Virus Research* (Thébault, S., ed.) pp. 1–38, Nova Science, Hauppauge, NY
5. Hall, W. W., and Fujii, M. (2005) *Oncogene* **24,** 5965–5975
6. Kashanchi, F., and Brady, J. N. (2005) *Oncogene* **24,** 5938–5951
7. Mesnard, J. M., and Devaux, C. (1999) *Virology* **257,** 277–284
8. Rousset, R., Fabre, S., Desbois, C., Bantignies, F., and Jalinot, P. (1998) *Oncogene* **16,** 643–654
9. Xie, L., Yamamoto, B., Haoudi, A., Semmes, O. J., and Green, P. L. (2006) *Blood* **107,** 1980–1988
10. Hirata, A., Higuchi, M., Niinuma, A., Ohashi, M., Fukushi, M., Oie, M., Akiyama, T., Tanaka, Y., Gejyo, F., and Fujii, M. (2004) *Virology* **318,** 327–336
11. Tsubata, C., Higuchi, M., Takahashi, M., Oie, M., Tanaka, Y., Gejyo, F., and Fujii, M. (2005) *Retrovirology* **2,** 46
12. Suzuki, T., Ohsugi, Y., Uchida-Toita, M., Akiyama, T., and Yoshida, M. (1999) *Oncogene* **18,** 5967–5972
13. Funke, L., Dakoji, S., and Bredt, D. S. (2005) *Annu. Rev. Biochem.* **74,** 219–245
14. Dimitratos, S. D., Woods, D. F., Stathakis, D. G., and Bryant, P. J. (1999) *Bioessays* **21,** 912–921
15. Round, J. L., Tomassian, T., Zhang, M., Patel, V., Schoenberger, P., and Miceli, M. C. (2005) *J. Exp. Med.* **201,** 419–430
16. Xavier, R., Rabizadeh, S., Ishiguro, K., Andre, N., Ortiz, J. B., Wachtel, H., Morris, D. G., Lopez-Ilasaca, M., Shaw, A. C., Swat, W., and Seed, B. (2004) *J. Cell Biol.* **166,** 173–178
17. Humbert, P., Russell, S., and Richardson, H. (2003) *Bioessays* **25,** 542–553
18. Lee, S. S., Weiss, R. S., and Javier, R. T. (1997) *Proc. Natl. Acad. Sci. U. S. A.* **94,** 6670–6675
19. Matsumine, A., Ogai, A., Senda, T., Okumura, N., Satoh, K., Baeg, G. H., Kawahara, T., Kobayashi, S., Okada, M., Toyoshima, K., and Akiyama, T. (1996) *Science* **272,** 1020–1023
20. Ishidate, T., Matsumine, A., Toyoshima, K., and Akiyama, T. (2000) *Oncogene* **19,** 365–372
21. Polakis, P. (1997) *Biochim. Biophys. Acta* **1332,** F127–F147
22. Kiyono, T., Hiraiwa, A., Fujita, M., Hayashi, Y., Akiyama, T., and Ishibashi, M. (1997) *Proc. Natl. Acad. Sci. U. S. A.* **94,** 11612–11616
23. McLaughlin, M., Hale, R., Ellston, D., Gaudet, S., Lue, R. A., and Viel, A. (2002) *J. Biol. Chem.* **277,** 6406–6412
24. Massimi, P., Gammoh, N., Thomas, M., and Banks, L. (2004) *Oncogene* **23,** 8033–8039
25. Bilder, D., Li, M., and Perrimon, N. (2000) *Science* **289,** 113–116
26. Nourry, C., Grant, S. G., and Borg, J. P. (2003) *Sci. STKE* **179,** 1–12
27. Mathew, D., Gramates, L. S., Packard, M., Thomas, U., Bilder, D., Perrimon, N., Gorczyca, M., and Budnik, V. (2002) *Curr. Biol.* **12,** 531–539
28. Ludford-Menting, M. J., Oliaro, J., Sarcibegovic, F., Cheah, E. T. Y., Pedersen, N., Thomas, S. J., Pasam, A., Iazzolino, R., Dow, L. E., Waterhouse, N. J., Murphy, A., Ellis, S., Smyth, M. J., Kershaw, M. H., Darcy, P. K., Humbert, P. O., and Russell, S. M. (2005) *Immunity* **22,** 737–748
29. Nakagawa, S., and Huibregtse, J. M. (2000) *Mol. Cell. Biol.* **2000,** 8244–8253
30. Gachon, F., Péléraux, A., Thébault, S., Dick, J., Lemasson, I., Devaux, C., and Mesnard, J. M. (1998) *J. Virol.* **72,** 8332–8337
31. Dow, L. E., Brumby, A. M., Muratore, R., Coombe, M. L., Sedelies, K. A., Trapani, J. A., Russell, S. M., Richardson, H. E., and Humbert, P. O. (2003) *Oncogene* **22,** 9225–9230
32. Gachon, F., Thebault, S., Peleraux, A., Devaux, C., and Mesnard, J. M. (2000) *Mol. Cell. Biol.* **20,** 3470–3481
33. Audebert, S., Navarro, C., Nourry, C., Chasserot-Golaz, S., Lécine, P., Bellaiche, Y., Dupont, J.-L., Premont, R. T., Sempéré, C., Strub, J.-M., Van Dorsselaer, A., Vitale, N., and Borg, J.-P. (2004) *Curr. Biol.* **14,** 987–995
34. Basbous, J., Bazarbachi, A., Granier, C., Devaux, C., and Mesnard, J. M. (2003) *J. Virol.* **77,** 13028–13035
35. Meertens, L., Chevalier, S., Weil, R., Gessain, A., and Mahieux, R. (2004) *J. Biol. Chem.* **279,** 43307–43320
36. Navarro, C., Nola, S., Audebert, S., Santoni, M.-J., Arsanto, J.-P., Ginestier, C., Marchetto, S., Jacquemier, J., Isnardon, D., Le Bivic, A., Birnbaum, D., and Borg, J. P. (2005) *Oncogene* **24,** 4330–4339
37. Hivin, P., Frédéric, M., Arpin-André, C., Basbous, J., Gay, B., Thébault, S., and Mesnard, J. M. (2005) *J. Cell Sci.* **118,** 1355–1362
38. Alefantis, T., Barmak, K., Harhaj, E. W., Grant, C., and Wigdahl, B. (2003) *J. Biol. Chem.* **278,** 21814–21822
39. Legouis, R., Bastard, F. J., Schott, S., Navarro, C., Borg, J. P., and Labouesse, M. (2003) *EMBO Rep.* **4,** 1096–1102
40. Kehn, K., De la Fuente, C., Strouss, K., Berro, R., Jiang, H., Brady, J. N., Mahieux, R., Pumfery, A., Bottazzi, M. E., and Kashanchi, F. (2004) *Oncogene* **24,** 525–540
41. Albertson, R., Chabu, C., Sheehan, A., and Doe, C. Q. (2004) *J. Cell Sci.* **117,** 6061–6070
42. Gardiol, D., Kuhne, C., Glaunsinger, B., Lee, S. S., Javier, R., and Banks, L. (1999) *Oncogene* **18,** 5487–5496
43. Nguyen, M. M., Nguyen, M. L., Caruana, G., Bernstein, A., Lambert, P. F., and Griep, A. E. (2003) *Mol. Cell. Biol.* **23,** 8970–8981
44. Takizawa, S., Nagasaka, K., Nakagawa, S., Yano, T., Nakagawa, K., Yasugi, T., Takeuchi, T., Kanda, T., Huibregtse, J. M., Akiyama, T., and Taketani, Y. (2006) *Genes Cells* **11,** 453–464
45. Davis, D. M., and Dustin, M. L. (2004) *Trends Immunol.* **25,** 323–327
46. Wilkinson, B., Wang, H., and Rudd, C. E. (2004) *Immunology* **111,** 368–374
47. de Waal Malefyt, R., Yssel, H., Spits, H., de Vries, J. E., Sancho, J., Terhorst, C., and Alarcon, B. (1990) *J. Immunol.* **145,** 2297–2303
48. Lemasson, I., Robert-Hebmann, V., Hamaia, S., Duc Dodon, M., Gazzolo, L., and Devaux, C. (1997) *J. Virol.* **71,** 1975–1983
49. Weil, R., Levraud, J. P., Dodon, M. D., Bessia, C., Hazan, U., Kourilsky, P., and Israel, A. (1999) *J. Virol.* **73,** 3709–3717
50. Hanada, T., Lin, L., Chandy, K. G., Oh, S. S., and Chishti, A. H. (1997) *J. Biol. Chem.* **272,** 26899–26904
51. Frese, K. K., Latorre, I. J., Chung, S. H., Caruana, G., Bernstein, A., Jones, S. N., Donehower, L. A., Justice, M. J., Garner, C. C., and Javier, R. T. (2006) *EMBO J.* **25,** 1406–1417